

Synthesis of Hyaluronan Haloacetates and Biology of Novel Cross-Linker-Free Synthetic Extracellular Matrix Hydrogels

Monica A. Serban and Glenn D. Prestwich*

Department of Medicinal Chemistry and Center for Therapeutic Biomaterials, The University of Utah,
419 Wakara Way, Suite 205, Salt Lake City, Utah 84108-1257

Received May 29, 2007; Revised Manuscript Received June 25, 2007

Hyaluronan (HA) derivatives containing thiol-reactive electrophilic esters were prepared to react with thiol-modified macromolecules to give cross-linker-free hydrogels. Specifically, HA was converted to two haloacetate derivatives, HA bromoacetate (HABA) and HA iodoacetate (HAIA). In cytotoxicity assays, these reactive macromolecules predictably induced cell death in a dose-dependent manner. Cross-linker-free synthetic extracellular matrix (sECM) hydrogels were prepared by thiol alkylation using HAIA and HABA as polyvalent electrophiles and thiol-modified HA (CMHA-S) with or without thiol-modified gelatin (Gtn-DTPH) as polyvalent nucleophiles. When primary human fibroblasts were seeded on the surface of the sECMs containing only the electrophilic HA haloacetate and nucleophilic CMHA-S components, no significant cytoadherence was observed. Cell attachment and viability was 17% (HABA) to 30% (HAIA) lower on HA haloacetate cross-linked hydrogels than on CMHA-S that had been oxidatively cross-linked via disulfide-bonds. In contrast, sECMs that included Gtn-DTPH allowed fibroblasts to attach, spread, and proliferate. Taken together, the HA haloacetates are attractive candidates for producing cross-linker-free sECM biomaterials that can function either as anti-adhesive barriers or as cytoadhesive sECMs for cell culture in pseudo-3-D.

Introduction

Hyaluronan (HA) is a ubiquitous and abundant non-sulfated glycosaminoglycan, first isolated in 1934 from the vitreous of bovine eyes.¹ Present in all vertebrates, it is a major component of the extracellular matrix (ECM),² and it is involved in vital processes such as cell differentiation,³ angiogenesis,^{4–7} morphogenesis,^{8,9} and wound healing.^{10,11} Because of its biological properties, HA has been extensively used in viscosurgery and viscosupplementation^{12–14} or as an adjuvant for ophthalmologic drug delivery.¹⁵ In addition, HA has excellent potential for constructing novel biocompatible scaffolds. However, chemical modification of HA is required to prepare covalently cross-linked hydrogels and to modulate *in vivo* degradation rates and cell attachment abilities of the resulting biomaterials. Chemically modified HA biomaterials are now used as major components of scaffolds for tissue engineering,^{16–21} soft and hard tissue repair,^{22–24} controlled drug release,^{17,25} and growth factor release.^{7,26–29} Many HA-based biomaterials are terminally modified or monolithic,³⁰ that is, they lack functionality for further chemical cross-linking under physiological conditions. Of the living HA derivatives that allow for further modifications, hydrazide^{31–33} and thiol-modified^{19,34,35} materials feature nucleophilic functionalities that can be cross-linked by polyvalent macromolecular electrophiles. One such biomaterial, HA-ADH, was obtained by modifying HA with adipic dihydrazide (ADH).³⁶ The pendant hydrazide groups of this macromolecule allow for further alterations, such as drug loading,³⁶ molecular probe labeling,³⁷ or cross-linking.³⁸ HA-ADH hydrogels cross-linked with electrophilic poly(ethylene glycol) (PEG) dialdehydes were successfully used for wound healing.^{31,32} Thiolated HA biopolymers obtained via a carbodiimide-mediated synthesis were cross-linked with electrophilic PEG

diacrylates (PEGDA) to yield hydrogels for tissue engineering applications.¹⁶

Only the acrylated^{39,40} and methacrylated analogues^{41,42} of HA qualify as electrophilic. For the most part, these (meth)acrylated HA analogues are employed for photoinitiated polymerization. For example, methacrylated HA solutions that were photocross-linked to yield clear patches were effectively used as sealants for corneal lacerations in rabbit models.⁴² In a separate study, photocross-linked glycidyl methacrylate-HA hydrogels were investigated for tissue engineering applications.⁴⁰ Conversely, methacrylated HA was chemically cross-linked with dithiothreitol (DTT) and loaded with erythropoietin and tested for sustained release *in vivo* and *in vitro*.⁴¹

We report here the synthesis and characterization of two novel electrophilic derivatives of HA. The new haloacetate derivatives of HA described herein offer inverted chemical reactivity relative to the thiol-modified HA derivatives, thereby conferring chemical reactivity toward polyvalent macromolecular nucleophiles. Since HA bromoacetate (HABA) and HA iodoacetate (HAIA) have different reactivities with thiol nucleophiles, both polymers were investigated in biological assays. The HA haloacetates contain thiol-reactive groups and thus show an expected mild cytotoxicity in cell culture at higher concentrations. However, the reaction of HABA or HAIA with polyvalent nucleophiles affords cytocompatible hydrogels. With thiol-modified HA derivatives, hydrogels that prevent cell attachment and spreading can be obtained. In contrast, by including a thiol-modified gelatin derivative as the macromolecular polynucleophile, cytocompatible hydrogels are produced that support attachment, spreading and proliferation of primary human fibroblasts. Thus, combining electrophilic and nucleophilic HA derivatives would provide novel hydrogels that could have potential uses in adhesion prevention and as non-immunogenic, non-inflammatory, and non-cytoadhesive coating materials for medical devices, such as stents and surgical implants.

* Corresponding author. E-mail: gprestwich@pharm.utah.edu.

Materials and Methods

Materials and Analytical Instrumentation. High molecular weight hyaluronan (HA, MW = 824 kDa) was from Contipro C Co., Czech Republic. Bromoacetic anhydride (BA) and hyaluronidase type I-S from bovine testes (HAse, 451 U/mg solid) were from Sigma-Aldrich Chemical Co., Milwaukee, WI. Phosphate buffered saline 10× (PBS), sodium hydroxide (NaOH), hydrochloric acid 12.1 N (HCl), sodium iodide (NaI), dibasic sodium phosphate, heptahydrate ($\text{Na}_2\text{PO}_4 \cdot 7\text{H}_2\text{O}$), and SpectraPor dialysis tubing MWCO 10,000 were from Fisher Scientific, Hanover Park, IL. SAMSAs fluorescein (5-((2-(and-3)-S-acetylmercapto)succinoyl)amino) fluorescein) mixed isomers were purchased from Molecular Probes Inc., Eugene, OR. T31 human tracheal scar fibroblasts were a generous gift from Dr. S. L. Thibeault (Division of Otolaryngology: Head and Neck Surgery, Department of Surgery, University of Utah, Salt Lake City, UT; Division of Otolaryngology: Head and Neck Surgery, Department of Surgery, University of Wisconsin, Madison, WI).

¹H NMR spectral data were acquired using a Varian INOVA 400 at 400 MHz. UV/vis spectra and measurements were performed on a Hewlett-Packard 8453 UV–visible spectrometer, Palo Alto, CA. Gel permeation chromatography (GPC) analysis was obtained using the following components: Waters 486 tunable absorbance detector, Waters 410 differential refractometer, Waters 515 HPLC pump, and Ultrahydrogel 1000 column (7.8 × 300 mm) (Waters Corp., Milford, MA). The mobile phase for GPC consisted of 0.2 M PBS buffer/methanol (80:20 volume ratio). The HA standards used to calibrate the system were from Novozymes Biopolymers, Bagsvaerd, Denmark. An OPTI Max microplate reader (Molecular Devices, Sunnyvale, CA) was used to determine the 490 nm absorbance values for cell viability assays.

Synthesis of Bromoacetate Derivatized Hyaluronan (HABA). Hyaluronan (6.0 g) was dissolved in 600 mL of distilled water (1% w/v solution). The pH of the solution was adjusted to 9.0 by adding 1 M NaOH. Bromoacetic anhydride (40 g, 153 mmol) was then added dropwise to the solution, and the reaction was stirred for 24 h at 4 °C. This amount of bromoacetic anhydride corresponds to 10 equiv relative to the number of primary C-6 hydroxyl groups of the *N*-acetylglucosamine residues. The reaction mixture was then dialyzed (MWCO 10000) for 3 days against distilled water. The sample was then lyophilized and analyzed. The purity of the sample was determined by ¹H NMR and GPC, and the degree of substitution (SD) was determined by derivatization with SAMSAs fluorescein (SD ~18%) (¹H NMR (D_2O); chemical shift corresponding to the substituent, $\delta = 3.84$ ppm (COCH_2Br)).

Synthesis of Iodoacetate Derivatized Hyaluronan (HAIA). HABA (2.15 g) was dissolved in 215 mL of distilled water (1% w/v solution) and reacted with 10 equiv of NaI. The reaction was stirred overnight at room temperature. Next, the reaction mixture was dialyzed for 3 days (MWCO 10000) and subsequently lyophilized. The purity of the modified hyaluronan was determined by ¹H NMR and GPC. The degree of substitution was calculated by SAMSAs fluorescein derivatization (SD ~19%) (¹H NMR (D_2O); chemical shift corresponding to the substituent, $\delta = 3.7$ ppm (COCH_2I)).

SAMSA Fluorescein Derivatization. SAMSAs fluorescein (25 mg) was dissolved in 2.5 mL of 0.1 M NaOH and incubated for 15 min at room temperature. HCl (6 N; 35 μL) was then added, followed by the addition of 0.5 mL of $\text{NaH}_2\text{PO}_4 \cdot \text{H}_2\text{O}$ at pH 7.0. HA-BA and HA-IA (5 mg of each) were reacted with activated SAMSAs fluorescein for 30 min at room temperature. The reaction mixtures were then separated on an Econo-Pac Bio-Rad column (Bio-Rad Laboratories, Hercules, CA) packed with Bio-Gel P-30 Gel with a nominal exclusion limit of 40 kDa (Bio-Rad Laboratories, Hercules, CA) to confirm covalent attachment. To determine the degree of derivatization for haloacetate HAs, the SAMSAs fluorescein–haloacetate HA reaction mixture was dialyzed for 3 days against dH_2O (MWCO 3500), and then, A_{494} was spectroscopically determined.

HA Haloacetate Cytotoxicity Assay. T31 human tracheal scar fibroblasts were seeded in 96-well plates at a density of 10^4 cells/mL

(100 μL /well) in DMEM/F12 + 10% newborn calf serum + 2 mM L-glutamine and incubated for 24 h at 37 °C/5% CO_2 . Stock solutions of 1.5% HABA, HAIA, and HA (120 kDa) were prepared in serum free, L-glutamine free growth medium, and the pH of solution was adjusted to 7.5–8 using 0.1 M NaOH. Solutions were then filtered through a 0.45 μm syringe driven filter unit to ensure sterility. The growth medium was then removed, and the cells were washed twice with 100 μL of serum free, L-glutamine free medium. Working solutions (100 μL of each 1.5%, 1%, 0.6%, 0.2%, and 0.1% in serum free, L-glutamine free medium) were added onto cells, and the plates were further incubated for an additional 24 h. Untreated cells were used as controls. Cell viability was assessed using the reduction of the tetrazolium compound MTS (Cell-Titer 96 Aqueous One Solution Cell Proliferation Assay, Promega, Madison, WI) to a colored formazan product.⁴³ The reduced salt has an absorbance maximum at 490 nm that can be monitored spectrophotometrically, and the intensity of the color is proportional to the number of viable cells in the well.

Gelation Studies. Thiol-modified carboxymethylated HA (CMHA-S, also known as Carbylan-S)⁴⁴ was used as the nucleophilic species in the reaction. This macromolecule had been synthesized by reaction of HA at high pH with chloroacetic acid to yield carboxymethylated HA (CMHA). CMHA was then further modified with 3,3'-di(thiopropionyl) bishydrazide (DTP) and subsequently reduced with dithiothreitol (DTT) to give CMHA-S.

The working solutions tested for gelation were 2% w/v CMHA-S, 2% w/v HABA, and 2% w/v HAIA solutions in 1× PBS at pH 7.0, 8.0, 9.0, 10.0, 11.0, and 12.0, adjusted by adding 1 M NaOH. The haloacetate HA-containing hydrogels were obtained by using a 3:1 nucleophile to electrophile molar ratio. The CMHA-S only hydrogels (control) were cross-linked through disulfide bonds by exposure to air. The solution (flowable liquid) to gel (non-flowing hydrogel) transition times were determined by the test tube inversion method.⁴⁵ The experiment was repeated three times, with consistent results.

Non-Adherent Hydrogels. Hydrogels consisting of CMHA-S and haloacetate HAs were obtained by dissolving 2% w/v solutions of CMHA-S, HABA, and HAIA (1× PBS, pH to 9.0) and mixing them in a 3:1 nucleophile to electrophile molar ratio after sterile filtration. The CMHA-S only hydrogels (control) were cross-linked through disulfide bonds by exposure to air. The composites were then cast in 96 well tissue culture plates and allowed to gel and cure in the hood at room temperature.

Cytoadherent Hydrogels. Cytoadherent hydrogels were obtained by adding thiol-modified gelatin (Gtn-DTPH) to the non-adherent hydrogels described above. Briefly, 2% w/v solution of Gtn-DTPH (1× PBS at pH 9.0) was mixed with 2% w/v CMHA-S (9:1 v/v), then reacted with 2% w/v haloacetate HA solutions (1× PBS at pH 9.0) in a 3:1 nucleophile to electrophile molar ratio after sterile filtration. The CMHA-S and Gtn-DTPH hydrogels (without haloacetate HAs) were cross-linked through disulfide bonds by exposure to air. As with the non-adherent gels, the composites were cast in 96-well tissue culture plates and allowed to gel and cure in the hood at room temperature. The gelation times for the Gtn-DTPH-containing biomaterials were similar to those of the non-adherent hydrogels.

Hydrogel Cytotoxicity Assay. Tissue culture plates (96-wells) were coated with 50 μL of CMHA-S, CMHA-S + HABA, CMHA-S + HAIA, CMHA-S + Gtn-DTPH, CMHA-S + Gtn-DTPH + HABA, and CMHA-S + Gtn-DTPH + HAIA hydrogels prepared at pH 9.0 and were allowed to cure overnight in hood. Uncoated wells were used as controls. Gels were then washed three times with 200 μL of medium (DMEM/F12 + 10% newborn calf serum) + 2 mM L-glutamine + penicillin/streptomycin, then cells (3.5×10^4 cells/mL) in the same medium were seeded in each well (100 μL /well). Cells were then incubated for 48 h at 37 °C/5% CO_2 . The colorimetric assay described above was used to assess the presence of viable cells. Cell attachment was verified microscopically, using an Olympus CKX41 microscope (Olympus America Inc., Melville, NY).

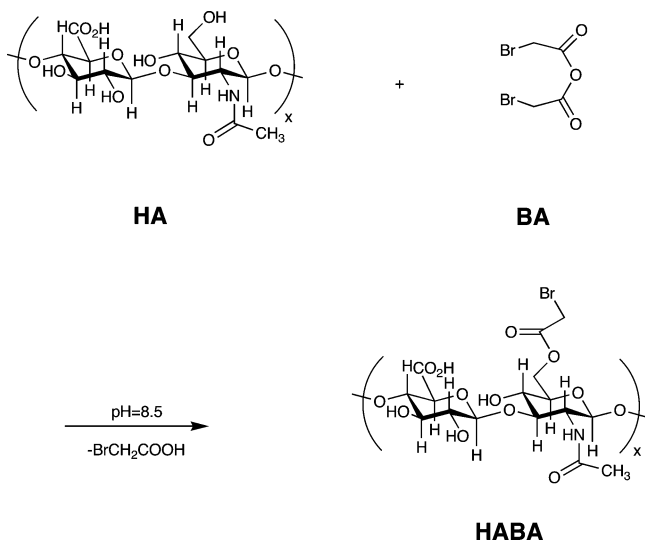


Figure 1. Synthetic scheme and structure of HABA.

Hydrogel Degradation. To determine the rate of enzymatic degradation of hydrogels in the presence of bovine testicular HASE (225 U/mL), 0.5 mL gels were cast in 17×60 mm glass vials (Fisher Scientific) and allowed to cure overnight. Subsequently, gels were covered with 600 μ L of $1 \times$ PBS at pH $7.4 \pm$ HASE and placed in an incubator at 37°C at 150 rpm. At predetermined time intervals, 300 μ L of PBS \pm HASE was removed, and A_{232} values were assessed spectrophotometrically (the absorbance range of oligosaccharides is 200–240 nm). For each time point, the supernatant removed for assaying was replaced with a fresh one (\pm HASE, as required). The absorbance value recorded 1 day after complete digestion was set as 100%, and absorbance values read on previous days were extrapolated to percentages.

Statistical Analysis. Values, represented as mean \pm standard deviation (S.D.) were compared using Student's *t*-test (2-tailed) with $p < 0.05$ considered statistically significant and $p < 0.005$ or $p < 0.001$ considered highly significant.

Results

Synthesis and Characterization of Bromoacetate-Derivatized HA (HABA). HABA was obtained by treating HA with bromoacetic anhydride under basic reaction conditions (Figure 1). The reactant molar excess is needed because of the formation of the mixed anhydride between bromoacetic anhydride and HA, which rapidly hydrolyzes to restore the HA glucuronic acid carboxylic acid groups. While this side reaction would not cause any interference with the overall biological activity of HABA, it consumes the anhydride reagent and reduces the overall bromoacetate modification of the primary hydroxyl groups. Subsequently, the reaction mixture was dialyzed to remove the hydrolyzed bromoacetic anhydride byproducts, sodium bromoacetate and sodium glycolate. The final product (HABA) was obtained at 78% yield by lyophilizing the frozen dialyzed solution.

The structure of HABA was confirmed by ^1H NMR in D_2O . Compared to the spectrum of the starting material (HA) (Figure 2A), a new broad resonance appeared at 3.84 ppm, corresponding to the methylene protons of the bromoacetate group (COCH_2Br) (Figure 2B). The purity and molecular weight distribution of HABA were determined by GPC (data not shown). The GPC profile was detected by both refractive index and UV and confirmed the purity of the compound. The molecular weight of the compound was determined to be MW ~ 120 kDa (polydispersity index 2.58), and the decrease in the

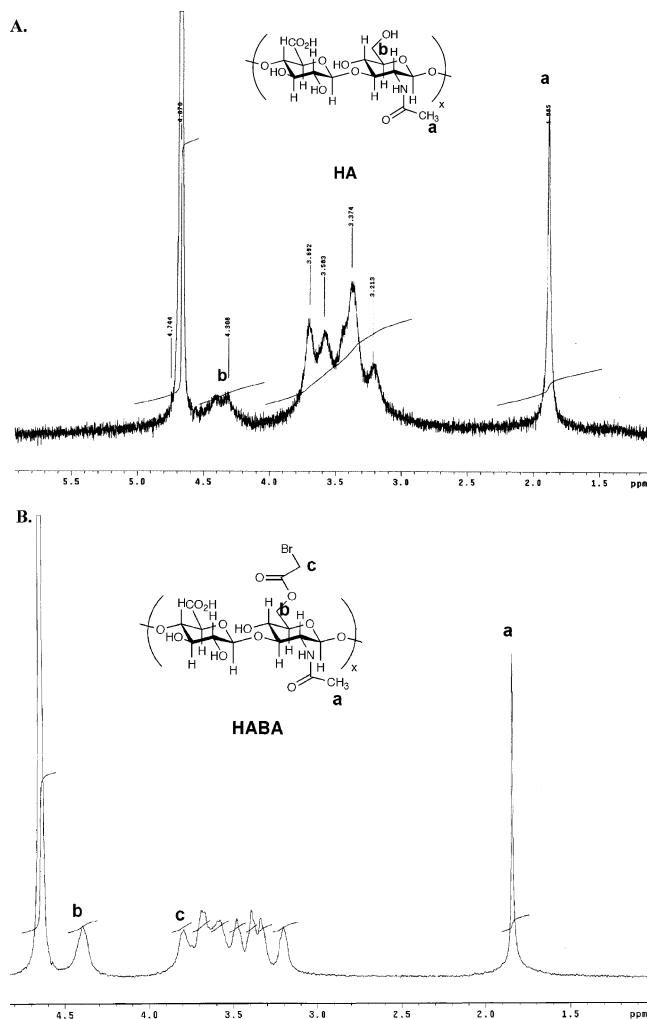


Figure 2. ^1H NMR spectra in D_2O . (A) HA and (B) HABA, showing a new peak at 3.84 ppm, corresponding to the methylene protons of the bromoacetate group (COCH_2Br).

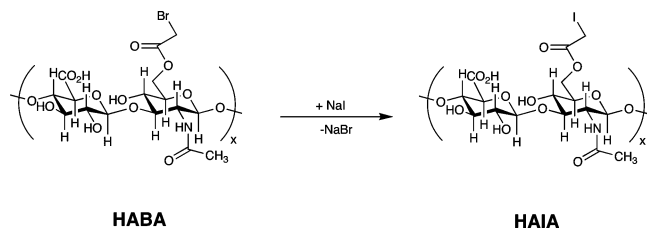


Figure 3. Synthetic scheme and structure of HAIA.

molecular weight (compared to that of the starting material) can be attributed to either basic or acidic hydrolysis during the course of the reaction and purification. The final HABA product is completely soluble in water. The substitution degree, defined as bromoacetate groups per 100 disaccharide units, was estimated by fluorescent dye derivatization to be approximately 18%.

Synthesis and Characterization of Iodoacetate-Derivatized HA (HAIA). The HABA obtained was divided into two equal batches. One batch was used for further chemical and biological characterization. The second batch was used as starting material for HAIA synthesis. HABA in nanopure water was reacted with NaI using a modified Finkelstein reaction (Figure 3), and the solution was dialyzed and lyophilized to give HAIA in 97% yield. Compared to the ^1H NMR spectrum of the starting HABA (Figure 2B), the peak corresponding to the methylene protons of the haloacetate group (COCH_2X , $\delta = 3.84$) shifted upfield

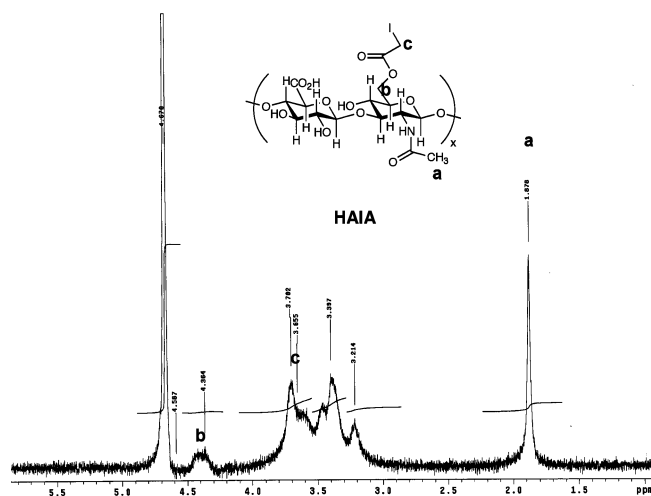


Figure 4. ^1H NMR spectrum in D_2O of HAIA. An enhanced peak at 3.7 ppm, corresponding to the iodoacetate group protons (COCH_2I) is observable.

to 3.70 ppm (Figure 4). GPC was employed to assess the purity and molecular weight distribution of HAIA (data not shown). The molecular weight of the compound was determined to be MW \sim 160 kDa (polydispersity index 2.45). The substitution degree was presumed to be identical to that of HABA because of the upfield shift of the ^1H NMR peak from $\delta = 3.84$ to $\delta = 3.70$ ppm.

SAMSA Fluorescein Derivatization of HA Haloacetates.

The gross structures of the two HA haloacetate derivatives were determined by ^1H NMR. However, because of the complexity of polymer proton spectra, an additional measure was used to test for successful chemical alteration. SAMSA fluorescein is a thiol group containing a fluorescent reagent, commonly used for assaying maleimide and iodoacetamide moieties of proteins (Figure 5A). Because of the nature of the novel reactive groups, SAMSA fluorescein derivatization was chosen to assess the presence and reactivity of the new moieties (bromoacetate for HABA and iodoacetate for HAIA). After conjugation of HA derivatives with SAMSA fluorescein as described under Materials and Methods and dialysis, the solutions were photographed under UV light to visually assess the fluorescence intensities (Figure 5B). The covalent attachment of the fluorescent moiety to HA haloacetates was further confirmed chromatographically (results not shown). The results of this experiment represent a proof of concept and show the successful chemical alteration of the HA polymer.

HA Haloacetate Cytotoxicity. Primary human tracheal scar T31 fibroblasts⁴⁶ were cultured in 96-well plates and were used as a model system to evaluate the effect of HABA and HAIA on non-immortalized primary cells. The cells were initially cultured in serum-containing medium to ensure proper growth. Subsequently, cells were washed with serum-free medium, and either HABA or HAIA at w/v concentrations of 1.5%, 1%, 0.6, 0.2%, and 0.1% in serum-free medium were added then to cells. Cells covered with serum-free medium only were used as controls. After 48 h, cell viability was assessed colorimetrically as described using the MTS assay. As expected for thiol-reactive electrophilic species, the two HA haloacetate polymers were cytotoxic at high concentrations. However, at low concentrations (0.1% w/v), they were well tolerated by these sensitive cells (Figure 6).

HA Haloacetate Cross-Linked Hydrogels. Figure 7 illustrates the two fundamentally different hydrogels prepared from the HA haloacetates. Thus, Figure 7A illustrates the

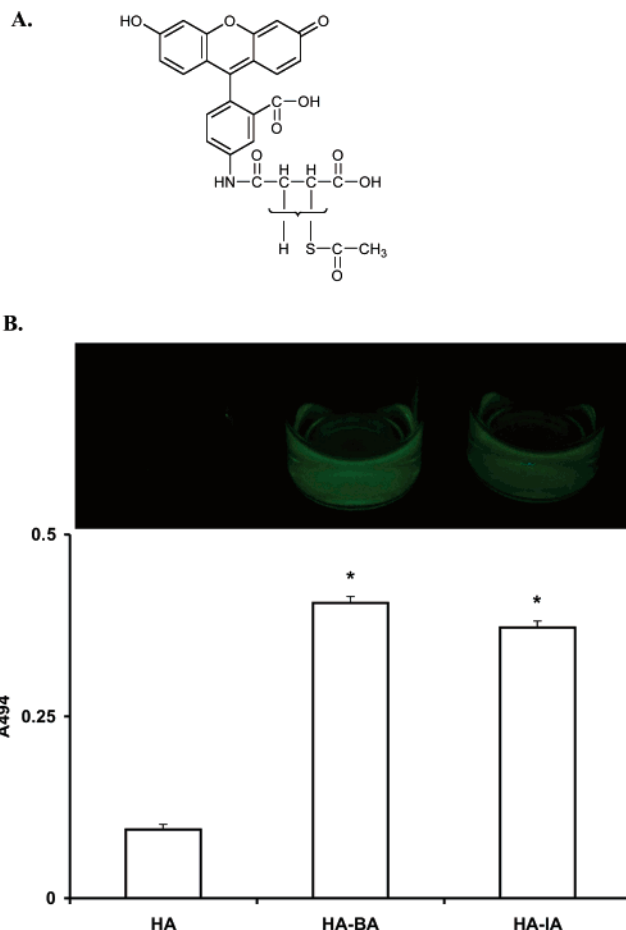


Figure 5. SAMSA fluorescein derivatization of haloacetate HAs. (A) Chemical structure of SAMSA fluorescein. (B) Quantitation of A_{494} absorbance values of SAMSA-derivatized compounds (* $p < 0.001$, vs the HA control). The columns represent the mean \pm S.D.; $n = 3$. (Inset) Fluorescence intensities of SAMSA derivatized solutions under UV light (254 nm).

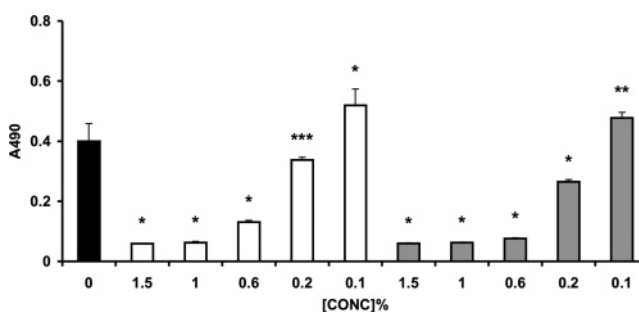


Figure 6. T31 fibroblast viability in the presence of haloacetate HAs. Black bar, untreated control; white bars, HABA treatment; gray bars, HAIA treatment (* $p < 0.005$, ** $p < 0.5$, and *** $p > 0.05$ vs untreated control). The columns represent the mean \pm S.D.; $n = 6$.

preparation of non-cyoadherent hydrogels based exclusively on two chemically modified HA derivatives, one electrophilic and one nucleophilic. Figure 7B shows that by incorporation of a thiol-modified gelatin derivative, the electrophilic and nucleophilic HA derivatives can be co-cross-linked into a cyoadherent hydrogel.

To determine the gelation time of haloacetate HA-containing biomaterials, hydrogels were prepared by mixing CMHA-S with HABA or HAIA in a 3:1 molar ratio. The pH dependence of gelation times was investigated next. Solutions (2% w/v) of CMHA-S and HABA or HAIA were made in $1\times$ PBS at pH 7.4, and the pH of the solutions was then adjusted to pH 7.0,

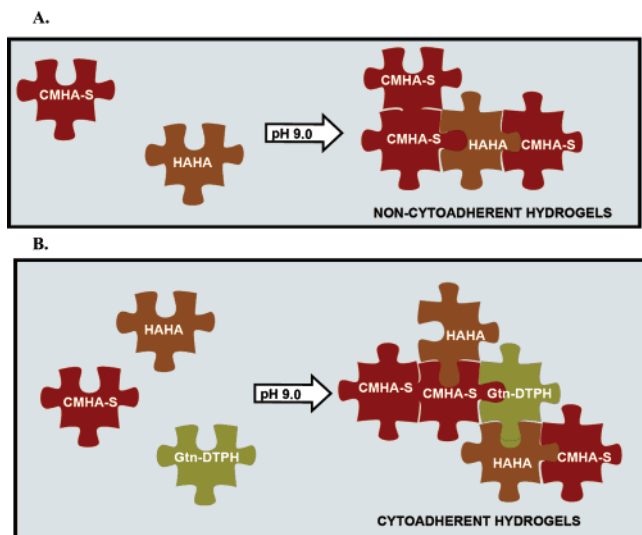


Figure 7. Schematic depiction of HA haloacetate-containing hydrogels. (A) Cross-linking of HA haloacetate with CMHA-S affords non-cytoadhesive hydrogels. (B) Cross-linking of HA haloacetate with CMHA-S and Gtn-DTPH affords cytoadhesive hydrogels.

Table 1. Gelation Times for the pH Dependent Gelation of Haloacetate HA Hydrogels

reactant		CMHA-S					
		gelation time (h)					
bromoacetate-HA (HABA)	28	7.5	2	2	7	23	
iodoacetate-HA (HAIA)	28	7.5	2	2	7	23	
CMHA-S	48	7	2	3	9	28	
pH		7	8	9	10	11	12

8.0, 9.0, 10.0, 11.0, and 12.0. As expected, the fastest setting solutions were those at pH 9.0 and 10.0 (Table 1). The gels obtained were clear and insoluble in aqueous solutions (data not shown). The gelation process of the haloacetate HA-containing hydrogels proceeds via a nucleophilic substitution reaction that leads to the formation of a thioether. The thiol groups of CMHA-S have a pKa value of approximately 9, which explains why the optimum pH for the reaction is 9–10.^{34,44} At lower pH values, the thiol group is mostly in its protonated form, while as the pH increases, the relative amount of the anionic nucleophile increases. At pH values above 10, hydroxide begins to displace iodide or bromide, making it unavailable for thioether formation.

Hydrogel Cytotoxicity. The non-cytoadherent hydrogels (Figure 7A) were prepared by mixing 2% w/v solutions of CMHA-S at pH 9.0 with 2% w/v solutions of HA haloacetates at pH 9.0 in a 3:1 molar ratio. The mixed solutions were then used to coat the wells of a 96-well plate and allowed to gel overnight in the hood. Before cell seeding, the hydrogels were washed with serum-containing medium, then 3.5×10^4 cells/mL (100 μ L/well) were seeded and incubated at 37 °C/5%CO₂ for 48 h.

Previous studies show that HA-based hydrogels such as Carbylan-SX do not promote cell adherence,^{16,47} while HA-based gels that contain a covalently cross-linked gelatin derivative support cell adherence and proliferation.¹⁹ To objectively evaluate the cytotoxicity of haloacetate HA-containing hydrogels, uncoated wells and wells coated with covalently linked gelatin (Gtn-DTPH)-containing gels were used as controls (Figure 7B). After 24 h, cells were examined microscopically. Cells seeded on Gtn-DTPH-free materials, were clustered

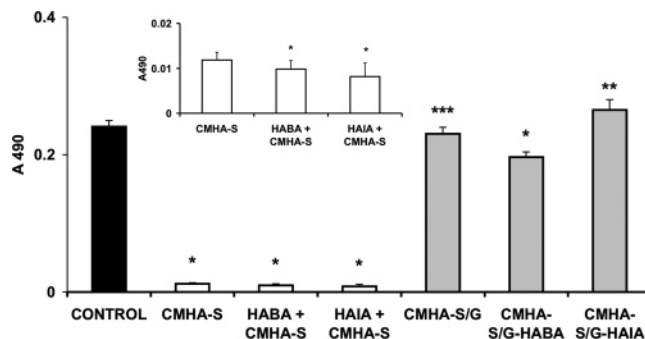


Figure 8. Viability of fibroblasts cultured on haloacetate HA hydrogels, as determined by MTS colorimetric assay. White bars, hydrogels without Gtn-DTPH; gray bars, hydrogels with Gtn-DTPH (* $p < 0.001$, ** $p < 0.05$, and *** $p > 0.05$ vs the control represented by a black bar). (Inset) Blow-up of A₄₉₀ values for fibroblasts cultured on Gtn-DTPH-free haloacetate HA hydrogels (* $p < 0.05$ vs CMHA-S). The values represented are the mean \pm S.D.; $n = 6$.

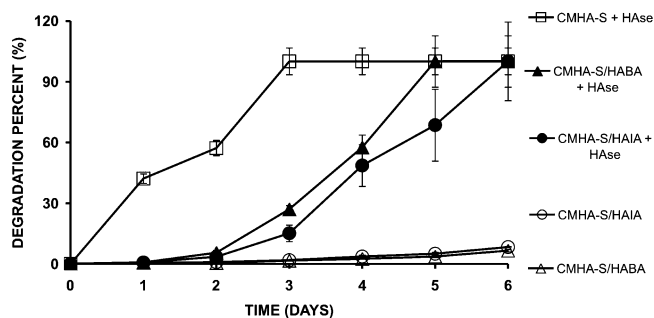


Figure 9. Hydrogel degradation rates in the presence or absence of Hase (225 U/mL). Each data point represents the mean \pm S.D.; $n = 3$.

together, rounded, and unattached, while cells grown on plastic only or on Gtn-DTPH-containing materials were spread out and elicited the typical spindle-shape morphology. Cellular viability was assessed by the MTS colorimetric assay, 48 h after cell seeding. In the absence of Gtn-DTPH, cells were not able to attach. Even fewer cells were present on haloacetate HA-containing gels, consistent with the cytotoxic effect of these materials (in hydrogels, the final haloacetate HA concentration is 0.67% w/v because a 2% w/v stock solution is added to the polymer solution at a 1:3 molar ratio) (Figure 8). Haloacetate HA-containing, Gtn-DTPH-free hydrogels showed 17% (HABA) to 30% (HAIA) decrease in cell adhesion/viability versus the control hydrogels (CMHA-S only) (see Figure 8, inset).

HA Haloacetate Hydrogel Degradation. The use of HA haloacetate hydrogels for medical purposes or any other *in vivo* application would be dependent on the rate of gel degradation under the action of hyaluronidases, which translates to the time that the coating material would actually be present *in vivo*. To estimate the rate of hydrogel degradation, Gtn-DTPH free hydrogels were incubated with $1 \times$ PBS at pH $7.4 \pm$ Hase (225 U/mL). Our results show that CMHA-S hydrogels that are cross-linked via disulfide bonds hydrolyze much faster than the HA haloacetate-containing materials (Figure 9). By the third day, CMHA-S hydrogels were totally degraded. In contrast, HABA-containing hydrogels appeared totally degraded by day 5, while CMHA-S/HAIA hydrogels degraded slightly slower (by day 6). In the absence of enzyme, HA haloacetate-containing hydrogels hydrolyze at a very slow rate. The hydrolysis rate for the CMHA-S-only hydrogel could not be determined due to the swelling of this hydrogel upon addition of supernatant, a behavior different from that of the HA haloacetate-containing gels.

Discussion

Previously, we described the chemical modification of HA with nucleophilic thiols that could be cross-linked with non-biological polyvalent electrophilic cross-linkers to yield hydrogels.^{48,49} Here, we sought to prepare a thiol-reactive electrophilic derivative of HA in order to prepare cross-linker-free hydrogels. To this end, reactive bromo and iodoacetate functionalities were introduced at the hydroxyl groups that are abundantly present on the HA polymer. HABA was prepared directly from HA and bromoacetic anhydride, but the use of iodoacetic anhydride for HAIA was avoided because of competing nucleophilic displacement of iodide by hydroxide under the basic conditions employed. Instead, HAIA was prepared from HABA by simple S_N2 substitution of bromide by iodide. As anticipated, the HA haloacetates showed a dose-dependent cytotoxic effect and tested with cultured T31 human tracheal scar fibroblasts. These primary human cells are more relevant for *in vivo* studies yet still capture the responses of fibroblastic cell lines that are often employed for *in vitro* biocompatibility and *in vitro* 3-D cytocompatibility experiments.

The reaction of HA haloacetates with nucleophilic macromolecules affords cytocompatible hydrogels. Depending on the composition, the hydrogels may either prevent or promote cell adherence, spreading, and proliferation. However, the prolonged gelation times of HA haloacetate-containing hydrogels make these impractical for most 3-D cell encapsulation protocols. Nevertheless, the hydrogels could be used for pseudo-3-D cultures, where cells would be seeded on top of hydrogels.

Similar, chemically modified HA hydrogels were fully degraded *in vitro* in 3 days in the presence of high levels of hyaluronidase.⁴⁹ The *in vivo* residence time of those subcutaneously implanted gels was determined to be more than 2 weeks.¹⁶ By analogy, our degradation data obtained under similar enzymatic conditions can be extrapolated to infer that HA haloacetate-containing hydrogels would have a residence time of approximately 4 weeks. The hyaluronidase concentration used in these *in vitro* assays was approximately 100-fold higher than the physiological enzyme units (ca. 2.6 U/mL in serum).⁵⁰

One potential application for the non-adherent HA haloacetate hydrogels could be adhesion prevention. Conditions such as bowel obstruction, pelvic pain, and even infertility can be the results of undesired post-surgical adhesions.⁵¹ Certain HA hydrogels have already been formulated to address this problem.⁵² For example, drug-loaded hydrogels such as mitomycin-C cross-linked HA hydrogels were successfully tested for adhesion prevention.⁵³ Sepafilim, a carbodiimide-modified HA/carboxymethyl cellulose-based material, has been clinically tested and proven to be successful in reducing adhesion formations after gynecological procedures.^{54,55} Carbylan-SX (PEGDA cross-linked CMHA-S hydrogel) has been shown to be effective in vocal fold repair by preventing scarring and ECM-based dysphonias.²⁵ In addition, this composite was used for post-operative intra-abdominal and abdominopelvic adhesion prevention.⁵⁶ HA haloacetate-based materials could further be used to improve the performance of currently available anti-adhesive biomaterials.

Medical device coating is another field that could benefit from the use of HA haloacetate-type biomaterials. Adsorption, ionic coupling, cross-linking, photochemical immobilization, covalent linking, and biospecific immobilization are common procedures used for HA coating of medical devices.⁵⁷ For example, endoluminal metallic stents, used for percutaneous coronary intervention, are commonly coated with biocompatible materials because of the significant incidence of in-stent restenosis in

patients who received non-coated stents (20% to 40% at 6 months after surgical intervention). Carbon-, silicon carbide-, gold-, or phosphorylcholine-coated stents were previously used for neointimal hyperplasia prevention.⁵⁸ Drug-coated stents that contained heparin⁵⁹ (antithrombotic), dexamethasone⁶⁰ (anti-inflammatory), or paclitaxel⁶¹ (anti-proliferative) were also developed. These coated materials were engineered to prevent or reduce thrombosis, inflammatory response, and aberrant cell adhesion and proliferation. Although promising, many of the coating materials induced neointimal hyperplasia, leading to restenosis and excessive inflammatory responses several months or even years after the surgical intervention.⁶²

The use of HA haloacetate-based coating materials could provide the awaited solution for restenosis prevention. Unmodified HA was already shown to be adherent to numerous scaffolds,^{63,64} and thus, we suggest that HA haloacetates could be just as easily immobilized on commonly used surgical scaffolds. In addition, the composition of HA haloacetate-based biomaterials would permit the modulation of post-surgical fibrotic responses. Their living structure would further allow for these materials to be chemically altered and tailored in an application-specific manner.

Conclusions

Two novel HA derivatives bearing haloacetate groups were successfully synthesized and characterized. Both materials elicit cytotoxic effects at high doses when added to normal cell culture medium. When the two new polymers were allowed to react with CMHA-S, a thiol-modified HA derivative, the hydrogels obtained did not support cell attachment and still elicited mild cytotoxic effects. In contrast, the co-cross-linking of CMHA-S plus Gtn-DTPH with HA haloacetates gave hydrogels that supported cell attachment and growth. Thus, the HA haloacetate platform offers access to both cytoadhesive materials or cytocompatible barriers to cell attachment. Moreover, HA haloacetate-containing hydrogels show slow Hase-mediated degradation rates, which make them suitable for *in vivo* applications. Taken together, our results suggest the adaptability and potential of the new materials for medical applications, specifically for adhesion prevention and medical device coating.

Acknowledgment. This research was supported by the State of Utah Centers of Excellence Program and by NIH Grant 2 R01 DC04336 (to S. L. Thiebault and G.D.P.). We also thank Dr. J. Anna Scott, Glycosan BioSystems, Inc., (www.glycosan.com), for providing the CMHA-S and Gtn-DTPH.

References and Notes

- (1) Meyer, K.; Palmer, J. W. The polysaccharide of the vitreous humor. *J. Biol. Chem.* **1934**, *107*, 629–634.
- (2) Knudson, C. B.; Knudson, W. Cartilage proteoglycans. *Semin. Cell Dev. Biol.* **2001**, *12*, 69–78.
- (3) Takahashi, Y.; Li, L.; Kamiryo, M.; Asteriou, T.; Moustakas, A.; Yamashita, H.; Heldin, P. Hyaluronan fragments induce endothelial cell differentiation in a CD44- and CXCL1/GRO1-dependent manner. *J. Biol. Chem.* **2005**, *280*, 24195–24204.
- (4) Forrester, J. V.; Balazs, E. A. Inhibition of phagocytosis by high molecular weight hyaluronate. *Immunology* **1980**, *40*, 435–446.
- (5) Goldberg, R. L.; Toole, B. P. Hyaluronate inhibition of cell proliferation. *Arthritis Rheum.* **1987**, *30*, 769–778.
- (6) Kujawa, M. J.; Carrino, D. A.; Caplan, A. I. Substrate-bonded hyaluronic acid exhibits a size-dependent stimulation of chondrogenic differentiation of stage 24 limb mesenchymal cells in culture. *Dev. Biol.* **1986**, *114*, 519–528.
- (7) Peattie, R. A.; Rieke, E. R.; Hewett, E. M.; Fisher, R. J.; Shu, X. Z.; Prestwich, G. D. Dual growth factor-induced angiogenesis *in vivo* using hyaluronan hydrogel implants. *Biomaterials* **2006**, *27*, 1868–1875.

- (8) Camenisch, T. D.; Schroeder, J. A.; Bradley, J.; Klewer, S. E.; McDonald, J. A. Heart-valve mesenchyme formation is dependent on hyaluronan-augmented activation of ErbB2-ErbB3 receptors. *Nat. Med.* **2002**, *8*, 850–855.
- (9) Toole, B. P. Hyaluronan in morphogenesis. *Semin. Cell Dev. Biol.* **2001**, *12*, 79–87.
- (10) Chen, W. Y.; Abatangelo, G. Functions of hyaluronan in wound repair. *Wound Repair Regen.* **1999**, *7*, 79–89.
- (11) Jia, C.; He, C.; Cherry, G. W.; Carbow, B.; Meyer-Ingold, W.; Bader, D.; West, D. C. Hyaluronan, heterogeneity, and healing: The effects of ultrapure hyaluronan of defined molecular size on the repair of full-thickness pig skin wounds. *Wound Repair Regen.* **1995**, *3*, 299–310.
- (12) Balazs, E. A.; Denlinger, J. L. Clinical uses of hyaluronan. *Ciba Found. Symp.* **1989**, *143*, 265–275; discussion 275–280, 281–285.
- (13) Davidson, J. M.; Nanney, L. B.; Broadley, K. N.; Whitsett, J. S.; Aquino, A. M.; Beccaro, M.; Rastrelli, A. Hyaluronate derivatives and their application to wound healing: preliminary observations. *Clin. Mater.* **1991**, *8*, 171–177.
- (14) Juhlin, L. Hyaluronan in skin. *J. Intern. Med.* **1997**, *242*, 61–66.
- (15) Saettone, M. F.; Monti, D.; Torracca, M. T.; Chetoni, P. Mucoadhesive ophthalmic vehicles: evaluation of polymeric low-viscosity formulations. *J. Ocul. Pharmacol.* **1994**, *10*, 83–92.
- (16) Hansen, J. K.; Thibeault, S. L.; Walsh, J. F.; Shu, X. Z.; Prestwich, G. D. In vivo engineering of the vocal fold extracellular matrix with injectable hyaluronic acid hydrogels: early effects on tissue repair and biomechanics in a rabbit model. *Ann. Otol., Rhinol., Laryngol.* **2005**, *114*, 662–670.
- (17) Langer, R. Biomaterials in drug delivery and tissue engineering: one laboratory's experience. *Acc. Chem. Res.* **2000**, *33*, 94–101.
- (18) Lee, K. Y.; Mooney, D. J. Hydrogels for tissue engineering. *Chem. Rev.* **2001**, *101*, 1869–1879.
- (19) Liu, Y.; Shu, X. Z.; Gray, S. D.; Prestwich, G. D. Disulfide-crosslinked hyaluronan-gelatin sponge: growth of fibrous tissue in vivo. *J. Biomed. Mater. Res., Part A* **2004**, *68*, 142–149.
- (20) Prestwich, G. D.; Shu, X. Z.; Liu, Y.; Cai, S.; Walsh, J. F.; Hughes, C. W.; Ahmad, S.; Kirker, K. R.; Yu, B.; Orlandi, R. R.; Park, A. H.; Thibeault, S. L.; Duflo, S.; Smith, M. E. Injectable Synthetic Extracellular Matrices for Tissue Engineering and Repair. In *Tissue Engineering*; Fisher, J., Ed.; Springer: New York, 2006; pp 125–134.
- (21) Yoo, H. S.; Lee, E. A.; Yoon, J. J.; Park, T. G. Hyaluronic acid modified biodegradable scaffolds for cartilage tissue engineering. *Biomaterials* **2005**, *26*, 1925–1933.
- (22) Duflo, S.; Thibeault, S. L.; Li, W.; Shu, X. Z.; Prestwich, G. D. Vocal fold tissue repair in vivo using a synthetic extracellular matrix. *Tissue Eng.* **2006**, *12*, 2171–2180.
- (23) Liu, Y.; Ahmad, S.; Shu, X. Z.; Sanders, R. K.; Kopesec, S. A.; Prestwich, G. D. Accelerated repair of cortical bone defects using a synthetic extracellular matrix to deliver human demineralized bone matrix. *J. Orthop. Res.* **2006**, *24*, 1454–1462.
- (24) Liu, Y.; Prestwich, G. D.; Shu, X. Z. Osteochondral defect repair with autologous bone-marrow derived mesenchymal stem cells in an injectable, in situ crosslinked synthetic extracellular matrix. *Tissue Eng.* **2006**, *12*, 3405–3416.
- (25) Liu, Y.; Li, H.; Shu, X. Z.; Gray, S. D.; Prestwich, G. D. Crosslinked hyaluronan hydrogels containing mitomycin C reduce postoperative abdominal adhesions. *Fertil. Steril.* **2005**, *83*, 1275–1283.
- (26) Cai, S.; Liu, Y.; Zheng, Shu, X.; Prestwich, G. D. Injectable glycosaminoglycan hydrogels for controlled release of human basic fibroblast growth factor. *Biomaterials* **2005**, *26*, 6054–6067.
- (27) Lee, K. Y.; Peters, M. C.; Anderson, K. W.; Mooney, D. J. Controlled growth factor release from synthetic extracellular matrices. *Nature* **2000**, *408*, 998–1000.
- (28) Liu, Y.; Cai, S.; Shu, X. Z.; Shelby, J.; Prestwich, G. D. Release of basic fibroblast growth factor from a crosslinked glycosaminoglycan hydrogel promotes wound healing. *Wound Repair Regen.* **2007**, *15*, 245–251.
- (29) Pike, D. B.; Cai, S.; Pomraning, K. R.; Firpo, M. A.; Fisher, R. J.; Shu, X. Z.; Prestwich, G. D.; Peattie, R. A. Heparin-regulated release of growth factors in vitro and angiogenic response in vivo to implanted hyaluronan hydrogels containing VEGF and bFGF. *Biomaterials* **2006**, *27*, 5242–5251.
- (30) Prestwich, G. D.; Kuo, J. W. Chemically-modified HA for therapy and regenerative medicine. *Curr. Pharm. Biotechnol.* **2007**, in press.
- (31) Kirker, K. R.; Luo, Y.; Morris, S. E.; Shelby, J.; Prestwich, G. D. Glycosaminoglycan hydrogels as supplemental wound dressings for donor sites. *J. Burn Care Rehabil.* **2004**, *25*, 276–286.
- (32) Kirker, K. R.; Luo, Y.; Nielson, J. H.; Shelby, J.; Prestwich, G. D. Glycosaminoglycan hydrogel films as bio-interactive dressings for wound healing. *Biomaterials* **2002**, *23*, 3661–3671.
- (33) Luo, Y.; Kirker, K. R.; Prestwich, G. D. Cross-linked hyaluronic acid hydrogel films: new biomaterials for drug delivery. *J. Controlled Release* **2000**, *69*, 169–184.
- (34) Shu, X. Z.; Liu, Y.; Luo, Y.; Roberts, M. C.; Prestwich, G. D. Disulfide cross-linked hyaluronan hydrogels. *Biomacromolecules* **2002**, *3*, 1304–1311.
- (35) Shu, X. Z.; Liu, Y.; Palumbo, F.; Prestwich, G. D. Disulfide-crosslinked hyaluronan-gelatin hydrogel films: a covalent mimic of the extracellular matrix for in vitro cell growth. *Biomaterials* **2003**, *24*, 3825–3834.
- (36) Pouyani, T.; Prestwich, G. D. Functionalized derivatives of hyaluronic acid oligosaccharides: drug carriers and novel biomaterials. *Bioconjugate Chem.* **1994**, *5*, 339–347.
- (37) Pouyani, T.; Prestwich, G. D. Biotinylated hyaluronic acid: a new tool for probing hyaluronate-receptor interactions. *Bioconjugate Chem.* **1994**, *5*, 370–372.
- (38) Vercruysse, K. P.; Marecak, D. M.; Marecek, J. F.; Prestwich, G. D. Synthesis and in vitro degradation of new polyvalent hydrazide cross-linked hydrogels of hyaluronic acid. *Bioconjugate Chem.* **1997**, *8*, 686–694.
- (39) Kim, J.; Kim, I. S.; Cho, T. H.; Lee, K. B.; Hwang, S. J.; Tae, G.; Noh, I.; Lee, S. H.; Park, Y.; Sun, K. Bone regeneration using hyaluronic acid-based hydrogel with bone morphogenic protein-2 and human mesenchymal stem cells. *Biomaterials* **2007**, *28*, 1830–1837.
- (40) Leach, J. B.; Bivens, K. A.; Collins, C. N.; Schmidt, C. E. Development of photocrosslinkable hyaluronic acid-polyethylene glycol-peptide composite hydrogels for soft tissue engineering. *J. Biomed. Mater. Res., Part A* **2004**, *70*, 74–82.
- (41) Hahn, S. K.; Oh, E. J.; Miyamoto, H.; Shimobouji, T. Sustained release formulation of erythropoietin using hyaluronic acid hydrogels crosslinked by Michael addition. *Int. J. Pharm.* **2006**, *322*, 44–51.
- (42) Miki, D.; Dastgheib, K.; Kim, T.; Pfister-Serres, A.; Smeds, K. A.; Inoue, M.; Hatchell, D. L.; Grinstaff, M. W. A photopolymerized sealant for corneal lacerations. *Cornea* **2002**, *21*, 393–399.
- (43) Lin, V. S.; Lee, M. C.; O'Neal, S.; McKean, J.; Sung, K. L. Ligament tissue engineering using synthetic biodegradable fiber scaffolds. *Tissue Eng.* **1999**, *5*, 443–452.
- (44) Prestwich, G. D.; Shu, X. Z.; Liu, Y. Modified Macromolecules and Methods of Making and Using Thereof. U.S. Patent 040726, 2004; World Patent 056608, 2005.
- (45) Jeong, B.; Bae, Y. H.; Kim, S. W. Thermoreversible gelation of PEG-PLGA-PEG triblock copolymer aqueous solutions. *Macromolecules* **1999**, *32*, 7064–7069.
- (46) Thibeault, S. L.; Li, W.; Gray, S. D.; Chen, Z. Instability of extracellular matrix gene expression in primary cell culture of fibroblasts from human vocal fold lamina propria and tracheal scar. *Ann. Otol., Rhinol., Laryngol.* **2002**, *111*, 8–14.
- (47) Sondrup, C.; Liu, Y.; Shu, X. Z.; Prestwich, G. D.; Smith, M. E. Cross-linked hyaluronan-coated stents in the prevention of airway stenosis. *Otolaryngol.—Head Neck Surg.* **2006**, *135*, 28–35.
- (48) Shu, X. Z.; Ghosh, K.; Liu, Y.; Palumbo, F. S.; Luo, Y.; Clark, R. A.; Prestwich, G. D. Attachment and spreading of fibroblasts on an RGD peptide-modified injectable hyaluronan hydrogel. *J. Biomed. Mater. Res., Part A* **2004**, *68*, 365–375.
- (49) Zheng, Shu, X.; Liu, Y.; Palumbo, F. S.; Luo, Y.; Prestwich, G. D. In situ crosslinkable hyaluronan hydrogels for tissue engineering. *Biomaterials* **2004**, *25*, 1339–1348.
- (50) Delpech, B.; Bertrand, P.; Chauzy, C. An indirect enzymoimmunological assay for hyaluronidase. *J. Immunol. Methods* **1987**, *104*, 223–9.
- (51) Diamond, M. P.; Freeman, M. L. Clinical implications of postsurgical adhesions. *Hum. Reprod. Update* **2001**, *7*, 567–576.
- (52) Ito, T.; Yeo, Y.; Highley, C. B.; Bellas, E.; Benitez, C. A.; Kohane, D. S. The prevention of peritoneal adhesions by in situ cross-linking hydrogels of hyaluronic acid and cellulose derivatives. *Biomaterials* **2007**, *28*, 975–83.
- (53) Li, H.; Liu, Y.; Shu, X. Z.; Gray, S. D.; Prestwich, G. D. Synthesis and biological evaluation of a cross-linked hyaluronan-mitomycin C hydrogel. *Biomacromolecules* **2004**, *5*, 895–902.

- (54) Burns, J. W.; Colt, M. J.; Burgees, L. S.; Skinner, K. C. Preclinical evaluation of Seprafilm bioresorbable membrane. *Eur. J. Surg.* **1997**, 40–48.
- (55) Burns, J. W.; Skinner, K.; Colt, J.; Sheidlin, A.; Bronson, R.; Yaacobi, Y.; Goldberg, E. P. Prevention of tissue injury and postsurgical adhesions by precoating tissues with hyaluronic acid solutions. *J. Surg. Res.* **1995**, 59, 644–652.
- (56) Liu, Y.; Shu, X. Z.; Prestwich, G. D. Reduced postoperative intra-abdominal adhesions using Carbylan-SX, a semisynthetic glycosaminoglycan hydrogel. *Fertil. Steril.* **2007**, 87, 940–948.
- (57) Morra, M. Engineering of biomaterials surfaces by hyaluronan. *Biomacromolecules* **2005**, 6, 1205–1223.
- (58) Babapulle, M. N.; Eisenberg, M. J. Coated stents for the prevention of restenosis: Part I. *Circulation* **2002**, 106, 2734–2740.
- (59) Gurbel, P. A.; Bliden, K. P. Platelet activation after stenting with heparin-coated versus noncoated stents. *Am. Heart J.* **2003**, 146, E10.
- (60) Lincoff, A. M.; Furst, J. G.; Ellis, S. G.; Tuch, R. J.; Topol, E. J. Sustained local delivery of dexamethasone by a novel intravascular eluting stent to prevent restenosis in the porcine coronary injury model. *J. Am. Coll. Cardiol.* **1997**, 29, 808–816.
- (61) Drachman, D. E.; Edelman, E. R.; Seifert, P.; Groothuis, A. R.; Bornstein, D. A.; Kamath, K. R.; Palasis, M.; Yang, D.; Nott, S. H.; Rogers, C. Neointimal thickening after stent delivery of paclitaxel: change in composition and arrest of growth over six months. *J. Am. Coll. Cardiol.* **2000**, 36, 2325–2332.
- (62) van der Giessen, W. J.; Lincoff, A. M.; Schwartz, R. S.; van Beusekom, H. M.; Serruys, P. W.; Holmes, D. R. Jr.; Ellis, S. G.; Topol, E. J. Marked inflammatory sequelae to implantation of biodegradable and nonbiodegradable polymers in porcine coronary arteries. *Circulation* **1996**, 94, 1690–1697.
- (63) Mason, M.; Vercruysse, K. P.; Kirker, K. R.; Frisch, R.; Marecak, D. M.; Prestwich, G. D.; Pitt, W. G. Attachment of hyaluronic acid to polypropylene, polystyrene, and polytetrafluoroethylene. *Biomaterials* **2000**, 21, 31–36.
- (64) Pitt, W. G.; Morris, R. N.; Mason, M. L.; Hall, M. W.; Luo, Y.; Prestwich, G. D. Attachment of hyaluronan to metallic surfaces. *J. Biomed. Mater. Res., Part A* **2004**, 68, 95–106.

BM700595S